Superpixel based Finger Vein ROI Extraction with Sensor Interoperability

Lu Yang, Gongping Yang*, Lizhen Zhou, Yilong Yin
School of Computer Science and Technology, Shandong University, Jinan, 250101, P.R. China
*Corresponding author: gpyang@sdu.edu.cn

Abstract

Finger vein is a new and promising trait in biometric recognition and some related progress have been achieved in recent years. Considering that there are many different sensors in a biometric system, sensor interoperability is a very important issue and still neglected in the state-of-the-art finger vein recognition. Based on the analysis of the shortcomings in the current finger vein ROI extraction methods, this paper proposes a new superpixel based finger vein ROI extraction method with sensor interoperability. First, finger boundaries are determined by tracking superpixels which are very robust to image variations such as gray level and background noises. Furthermore, to handle finger displacement, the middle points of the detected finger boundaries are used to adjust finger direction. Finally, finger ROI is localized by the internal tangents of finger boundaries. Experimental results show that the proposed method can extract the ROIs accurately and adaptively from images which are captured by different sensors.

1. Introduction

Finger vein recognition, a new physiological biometric technique, uses vein pattern in human finger to perform identity authentication. Comparing to the traditional biometric traits (*i.e.*, face, fingerprint, voice, *etc.*), it has distinctive advantages in living-body identification and internal characteristic. In recent years, finger vein has attracted lots of research effort, and some progress have been achieved [8, 9, 3].

ROI (region of interest) extraction is one important preprocessing step in finger vein recognition, and many related methods have been developed in previous literatures. These methods can be roughly grouped into the following four types: (I) predefined window based method [15], (II) sobel operator based method [16], (III) masks based method [7], and (IV) threshold based method [3]. All the existing methods achieve good performance on the database captured by one sensor. But in practical application, multiple image acquisition sensors may be used in one finger vein recognition system. And it is unavoidable that variations about image size, gray level and background noise exist in images from different sensors. These differences will degrade the performance of the existing ROI extraction methods. In detail, predefined window based method cannot accommodate to the change of finger size and image size. The illumination and gray level variations will affect threshold based method. In addition, sobel operator based method and masks based method have no robustness to background noise. In one word, these methods may not be able to deal with images from different sensors.

The ability of a biometric system to adapt to the new data obtained from a variety of sensors was named sensor interoperability [11]. The impact of sensor variation on fingerprint matching performance was illustrated [11]. And, some methods have been proposed to overcome this problem, including a thin-plate spline calibration model [12], a decision tree based segmentation [4], a hierarchical registration algorithm [18] and so on. Besides, the problem of sensor interoperability in iris recognition was also concerned and many approaches have been proposed to mitigate the cross-sensor recognition performance degradation [14, 2, 10]. But, it is a pity that there is no literature exploring sensor interoperability in finger vein recognition.

In this paper, we verify that the cross-sensor finger vein ROI extraction is indeed a challenge for finger vein recognition, and propose a superpixel based method to address this issue. In the proposed method, superpixel over-segmentation is used to group finger vein image into superpixels, and the grouped superpixels will be tracked to detect finger boundary. To remove the detected wrong boundaries, we further conduct the sobel operator based post-processing. And then, according to the middle points of finger boundaries, we adjust finger direction for images with finger displacement. Last, ROI is localized by the internal tangents of finger boundaries.

The rest of the paper is organized as follows: Section 2 analyzes the problem of sensor interoperability in finger vein ROI extraction. Next, the proposed method is described in Section 3, and Section 4 reports the experimental results. Finally, the conclusions of this paper are drawn in

Table 1. Some public finger vein databases

Database	Acquisition way	Finger number	Image number per finger	Image size(pixels)
SDUMLA-FV [17]	light transmission	636	6	320×240
HKPU-FV [3]	light transmission	312	12/6*	513×256
MMCBNU_6000 [6]	light transmission	600	10	640×480
UTFV [13]	light transmission	360	4	672×380

*Some fingers each has 12 images, and the others each has 6 images.

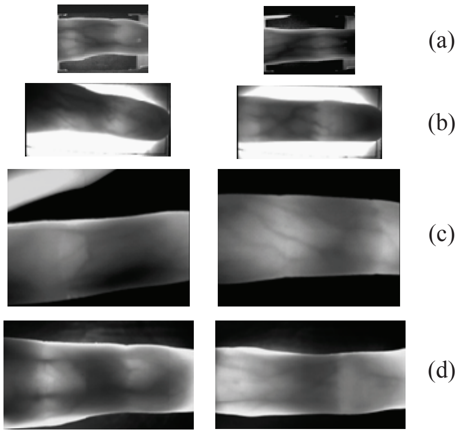

Figure 1. Some typical images from different databases. (a): from SDUMLA-FV; (b): from HKPU-FV; (c): from MMCBNU_6000; (d): from UTFV.

Section 5.

2. Problem Analysis

Finger vein can be captured by near-infrared light with wavelengths between 700 and 1,000 nanometers. The principle is that, near-infrared light can be absorbed intensively by the hemoglobin in the blood of vein, but transmits other tissues of finger easily, therefore vein pattern in finger will be captured as shadows. And there are two methods of image acquisition, *i.e.*, light reflection method and light transmission method. Although most of existing sensors adopt the second method, images from different sensors still have obvious differences. The main reason may be that there is no uniform sensor manufacture rule, such as different sensors may use different light sources and cameras.

Table 1 describes some public finger vein databases captured by different sensors, and some typical images from these databases are shown in Figure 1. From the table and the figure, we can see that the differences between images from different sensors mainly focus on three points, *i.e.*, image size, the gray level of image background, and the noise of image background. In detail, the size of image varied greatly. And the gray level of background in the second image is relatively high, but it in other images is low. Besides, the first two images have lots of noises in background, but there are fewer noises in background of the last two images. In these differences, the gray level and noises in image background will influence the finger boundary detection seriously.

Considering the differences in images from multiple sensors, the existing ROI extraction methods unavoidably have some shortcomings in handling these images. The sensor interoperabilities of the existing methods are analyzed in the following:

(I) Predefined window based method. In this kind of method, the size of the predefined window is usually fixed, which determines that the method cannot adapt to the change of image size.

(II) Sobel operator based method. The distribution and shape of background noises are quite different in images from different sensors, and relatively speaking, sobel operator is sensitive to noises. So, it will be not easy to denoise from finger boundary detected by sobel operator.

(III) Masks based method. In this kind of method, the predefined mask is filtered with the first or second half of the original image column by column, and the pixel with the maximum response value in one column will be regarded as finger boundary point. The method cannot work well in images with noises. For example, the noise boundary will be wrongly regarded as finger boundary in the first image of Figure 1(c), as the pixel on the noise border will have the maximum response value.

(IV) Threshold based method. If all the pixels in image background have lower or higher gray value than the pixels in finger area, a predefined threshold may be enough for ROI localization. But, it is very hard to avoid that the local finger area has similar gray value with image background. So, this kind of method generally cannot work well even on images from one sensor, let alone images from multiple sensors.

The above analysis indicates that it is very essential to design a cross-sensor ROI extraction method to deal with images from multiple sensors adaptively.

3. Proposed Method

In finger vein ROI extraction, finger boundary detection is the most important step, so a cross-sensor ROI extraction

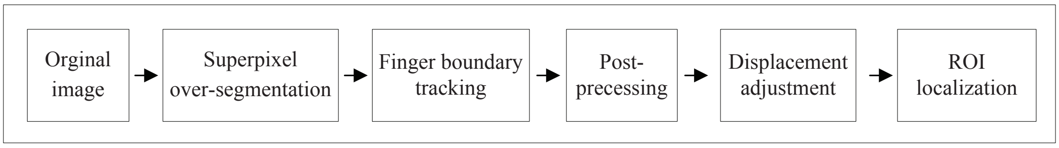

Figure 2. Block diagram of main steps in the proposed method.

method demands that the finger boundary detection method is robust to image variations. Fortunately, the superpixel over-segmentation method is insensitive to image variations to a certain degree. What's more, the method groups nearby pixels by enforcing local consistency, so finger area and image background can be generally segmented into different superpixels. Therefore, tracking finger boundary from superpixel over-segmented image may be a practicable way. And the shape of the tracked finger boundary is used to decide if the post-processing is needed. In post-processing, sobel operator will be used to detect finger boundary from the finger area localized by the tracked finger boundary.

Additionally, as the random finger placement during image acquisition, finger displacement exists in some images. For this kind of images, finger displacement adjustment is conducted according to the middle points of the detected finger boundaries. Last, ROI will be localized based on the internal tangents of finger boundaries. Figure 2 illustrates the main steps involved in the proposed method.

3.1. Finger Boundary Detection

In this section, we describe the superpixel and sobel based finger boundary detection method. In detail, finger boundaries are tracked from single pixel based superpixel boundary, and the sobel based post-processing is conducted for some images, whose tracked finger boundaries are wrong. The method can be divided into four sub-steps, which are introduced in the following:

(I) Superpixel over-segmentation: We use the simple linear iterative clustering (SLIC) method [1, 5] to conduct finger vein superpixel over-segmentation. The SLIC method uses the local intensity and position information to segment an image into small patches, and the segmented superpixels has good adherence to image boundaries. Some segmented finger vein images are illustrated in Figure 3. From the figure, we can see that the boundaries of superpixels adhere to finger boundaries well, and one boundary of superpixels on finger border is parallel to finger. But, the other boundaries are vertical or show a tilt angle to finger. So, finger boundary can be sought out by tracking the boundaries of superpixels along finger.

(II)Tracking point selection: The initial point of boundary tracking is named the tracking point. The tracking point selection is the basis of finger boundary tracking. Only if the selected tracking point is located on the finger boundary, the accurate finger boundary can be detected. By the observation to the images, we discover that the middle area of image is almost noise-free, so sobel operator is used to detect finger boundary from this area. And, we randomly select the tracking point from the overlapped points between the superpixel boundary and the boundary detected by sobel operator. Two kinds of boundaries and the overlapped points are shown in Figure 4.

(III)Finger boundary tracking: The boundary tracking operation starts from the randomly selected tracking point.

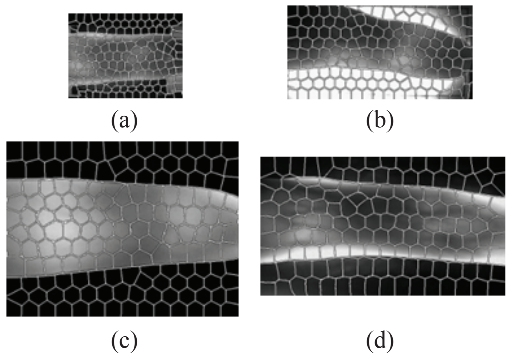

Figure 3. Superpixel over-segmented images. (a),(b),(c),(d) are from the four databases introduced in Table 1.

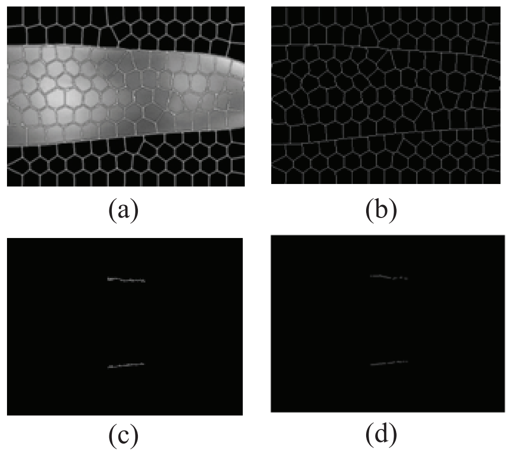

Figure 4. Selection of the tracking point. (a)Superpixel over-segmented image; (b) Superpixel boundaries; (c) Finger boundary detected by sobel operator; (d) Overlapped points.

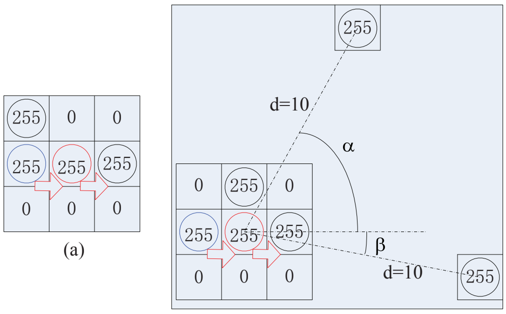

(b)

Figure 5. Tracking criteria. (a) Not backtrack; (b) Neighbor point with the smaller angle first. The blue circle means the tracked point; the red one is the current point; the black ones are neighbor points of the current point. And the red arrow means the tracking direction.

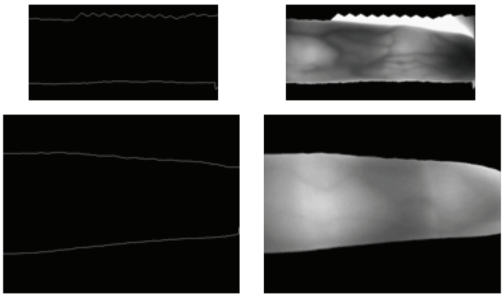

(a) (b)

Figure 6. (a) Tracked finger boundary; (b) Corresponding finger area.

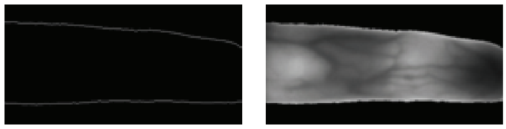

(a) (b)

Figure 7. (a) Post-processed finger boundary; (b) Corresponding finger area image.

The current pixel position is called the current point, and it moves pixel by pixel along finger from the tracking point to the fingertip and finger root, separately. And the next point is selected from eight neighbors of the current point. If the neighbor of the current point is on the superpixel boundary, we call it boundary neighbor, and it will be the candidate of the next point. Some tracking criteria are defined to select the optimal next point:

(i) Go to the only neighbor. If the current point has only one boundary neighbor, the neighbor will be the next point.

(ii) Not backtrack. If the left and right sides of the current point all have boundary neighbors, tracking direction will determine which neighbor will be selected. For example, the current point moves to the right side of image (*i.e.*, fingertip side), the neighbor on the right side of the current point has priority to be the next point, as shown in Figure 5(a).

(iii) Neighbor point with the smallest horizontal angle first. It means that, when the current point has multiple neighbors and the neighbors are located on the same side of the current point, the neighbor with the smallest horizontal angle will be tracked. One example is shown in Figure 5(b). In the figure, two boundary neighbors will be tracked separately until the dth neighbor of the current point. And then, the horizontal angle of the line between the current point and the dth neighbor will be calculated. As the finger is placed in horizontal direction, the neighbor with the smaller horizontal angle will be the next point.

Some tracked finger boundary and the corresponding localized finger area are shown in Figure 6. The figure shows that the accurate finger boundaries are detected in one image, but the boundaries in the other image are wrong. The wrong result may caused by the imperfect tracking point. For the wrong result, post-processing will be performed further.

(IV) Post-processing: We need to pick out the wrong finger boundary, and then conduct post-processing for this kind of images. From Figure 6, we can see that the accurate finger boundary is a relatively smooth curve, but the wrong one has a wavy shape. In smooth curve, the row numbers of all boundary points are nearly equal, but in a wavy shape, the row number goes up and down repeatedly. Therefore, the difference about the row number variation of boundary points is used to decide if the image needs further post-processing. But, even in a wavy shape, row numbers of two neighbor points is almost equal, which is same to the smooth curve. So, the step is set to 15 in the calculation of the row number variation. The calculation is shown in Formula 1:

$$D(i) = abs(\frac{row(i) - row(i+15)}{15}), \mathrm{i} = 1, ..., \mathrm{n} - 15 \tag{1}$$

where row saves the row number of all boundary points, n is the number of boundary points. If the element value in D is bigger than the predefined threshold, the detected boundary may has a wavy shape, and post-processing will be performed for it.

For the wrong finger boundary, such as the first image in Figure 6(b), sobel operator is used to detect finger boundary from the localized finger area, not from the original image. The reason is that the localized finger area has fewer noises than the original image. The post-processed finger boundary and corresponding localized finger area are shown in Figure 7.

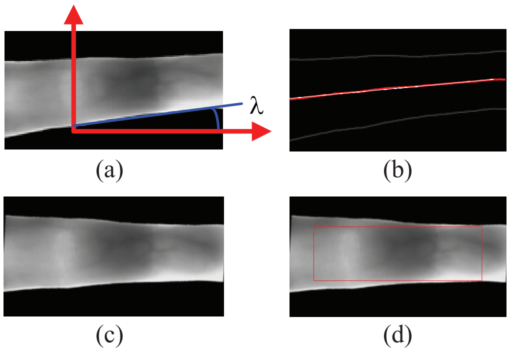

Figure 8. Finger displacement adjustment and ROI localization. (a) Original image; (b) Synthesized line (in red); (c) Adjusted image; (d) Localized ROI (in red rectangle).

3.2. Finger displacement Adjustment and ROI Localization

Due to the random finger placement during image acquisition, there is a certain amount of images, in which fingers do not parallel the X-axis. This kind of finger displacement will cause the loss of a portion of finger area in ROI extraction. So, in this section, we will find out these images and adjust finger displacement. And, finger ROI will be extracted from the adjusted image.

We use the middle points of two detected finger boundaries to adjust finger displacement as [16]. First, the middle points of two finger boundaries are computed and synthesized into a straight line, denoted by Formula 2:

$$y = a \times x + b \tag{2}$$

where a is the slope coefficient of the line. Second, the slope coefficient is utilized to compute the angle between finger direction and the X-axis:

$$\lambda = \frac{\arctan(a) \times 360}{2\pi} \tag{3}$$

Last, the finger displacement is adjusted according to the computed angle λ. The process of adjustment is shown in Figure 8(a), (b), (c).

As most of vein patterns actually disappear at the fingertip and finger root area in images, we cut off ten percent of the height of finger from the fingertip and finger root area of the images. And then, we localize the area between the internal tangents of two finger boundaries to obtain ROI. Figure 8(d) gives the localized ROI image.

4. Experimental Results

To ascertain the effectiveness of the proposed method, three experiments are designed on the introduced four public finger vein databases, including the presentation of the ROI extraction results, the performance comparison of different finger boundary detection methods, and the area measurement of the extracted ROI.

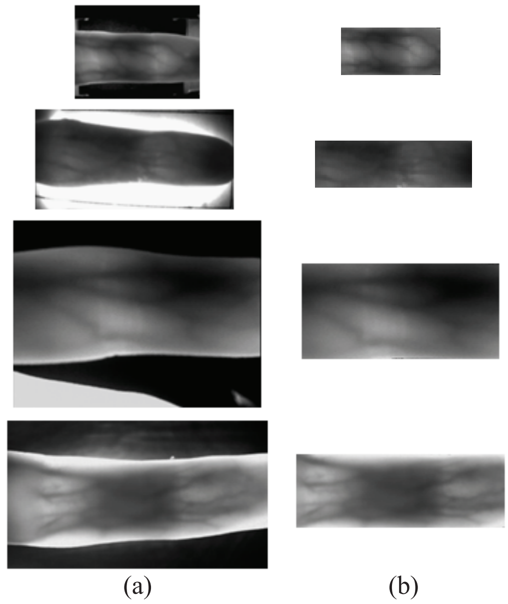

Figure 9. Some typical images and corresponding ROIs. (a) Original images; (b) ROIs.

4.1. Typical ROI Extraction Results

To prove the sensor interoperability of the proposed method, we present some extracted ROIs in this section. One typical image is selected from each database as examples to show the corresponding ROIs. The selected images have some variations in image size, background gray level and background noises, which can reflect the image variations from multiple sensors. Additionally, finger displacement also exists in some images. The selected images and the corresponding ROIs are shown in Figure 9.

From the figure, we can see that the accurate ROI can be extracted from all images. The success of the proposed method principally owes to superpixel based finger boundary tracking and finger displacement adjustment. In detail, the finger boundary tracking method is robust to image variations, and the displacement adjustment method can effectively correct finger displacement. In one word, the proposed method can effectively extract accurate finger ROIs form images captured by multiple sensors.

4.2. Comparison on Finger Boundary Detection

In this section, we study the performance of all kinds of finger boundary detection methods. The proposed finger boundary detection method is compared with three existing methods, *i.e.*, sobel operator based method, masks based method and threshold based method. In masks based

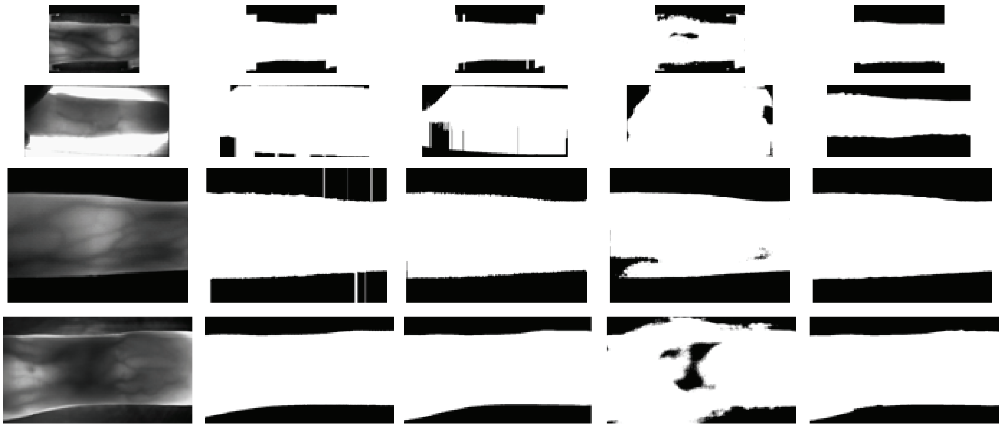

Figure 10. Comparison of finger boundary detection.

method, the masks defined in [7] are used, and considering the low background gray level in most selected images, the threshold is set 40 in threshold based method.

One typical image is selected from each database as examples to show the detected results. To clearly and intuitively show the detected finger boundaries, the original image is binarized according to the finger boundaries. In detail, the image area inside the finger boundaries is filled with gray value 255 to denote finger area, and the outside area is filled with gray value 0 to denote image background. The original images and the corresponding binarized images are shown in Figure 10.

The experimental results show that the proposed finger boundary detection method not only achieves the best results on all selected images, but also has robust sensor interoperability. The figure also reveals that, masks based method achieves the good results on the last two images, but on the other images, background noises cause the degradation of its performance. Besides, the rest two methods do not perform well on most of images. The performance of sobel based method is highly influenced by the noises in image background. For example, the block lines on the top and bottom of the second image are treated as finger boundaries. And the bad results of threshold based method are caused by the fact that local finger area has lower gray level than the predefined threshold as image background. What's worst, the whole area of the second image is nearly regarded as finger. This is due to the image background also has larger gray value than the predefined threshold.

In addition, the experimental results also suggest that the finger boundary detection of the last two images is relatively easier than the first two images. The main reason is that the complicated background noises in the first two images make finger boundary detection method failed.

Table 2. Comparison of ROI area.

ROI types	Area rate (%)
AUTO_ROI / MANUAL_ROI	0.9644
DIS_ROI / MANUAL_ROI	0.8074
DIS_ROI / AUTO_ROI	0.8372

4.3. Measurement of ROI Area

We measure the area of the ROIs, which are extracted in three different cases. In detail, the ROIs in different cases includes: (1) the automatically extracted ROI with finger displacement adjustment, denoted by AUTO_ROI; (2) the automatically extracted ROI without finger displacement adjustment, denoted by DIS_ROI; and (3) the manually extracted ROI, denoted by MANUAL_ROI. The comparison between the first and the second cases are used to evaluate the effectiveness of finger displacement adjustment, and the third case is used to verify if the more finger vein patterns can be extracted by the proposed method. The randomly selected 50 images with finger displacement are used to conduct this experiment. The average area ratio between ROIs, extracted in different cases, is given in Table 2. And the extracted ROIs of two typical images with finger displacement are shown in Figure 11.

The area ratio between ROIs, extracted by the proposed method and the expert, is 96.44%. It means that the proposed method extracts smaller useful finger area compared with the expert. The main reason is that we cut off the areas of fingertip and finger root in all images, but the expert can subjectively retain these two areas if the areas are filled with the clear vein patterns. From the table, we also can see that the extracted ROI from images without finger displacement adjustment has the minimum area. It is due to that the fin-

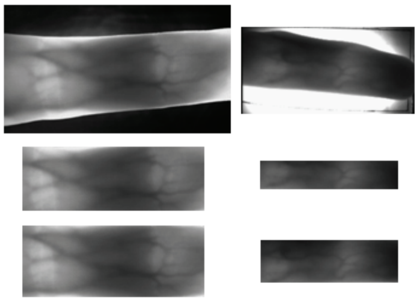

(a)

(b)

(c)

Figure 11. Original images and corresponding ROIs. (a) Original images; (b) ROIs without displacement adjustment; and (c) ROIs with displacement adjustment.

ger area between two internal tangents of finger boundaries is very small in images with finger displacement. And, it also can prove that finger displacement adjustment is helpful for ROI extraction. In addition, Figure 11 shows the similar results, and we see that the areas of ROIs in subfigure (b) are smaller than those of ROIs in subfigure (c).

5. Conclusions

In this paper, we present a new ROI extraction method, which can handle images from multiple sensors. In the method, the superpixel based finger boundary detection is robust to image variations such as image size, gray level, background noise. And finger displacement adjustment can make more finger area be extracted. Based on the superpixel based finger boundary detection and the finger displacement adjustment, the proposed method can extract ROIs accurately and adaptively from images captured by multiple sensors.

However, the wrong finger boundaries are detected in some images. This is mainly due to the imperfect tracking point. The similar gray level between finger border and image background leads to the bad adherence of superpixels to finger boundary. In this case, the selected tracking point is always not on the finger boundary. So, how to select the perfect tracking point may be one worthy future work. In addition, we also plan to explore the finger vein matching method with sensor interoperability.

6. Acknowledgements

The work is supported by National Science Foundation of China under Grant No.61173069, 61472226 and Shandong Natural Science Funds for Distinguished Young Scholar under Grant No. JQ201316. The authors would like to thank the anonymous reviewers for their helpful suggestions.

References

[1] R. Achanta, A. Shaji, K. Smith, A. Lucchi, P. Fua, and S. Susstrunk. Slic superpixels compared to state-of-the-art superpixel methods. *IEEE Transactions on Pattern Analysis and Machine Intelligence*, 34(11):2274–2282, 2012.

[2] S. S. Arora, M. Vatsa, R. Singh, and A. Jain. On iris camera interoperability. In *2012 IEEE Fifth International Conference on Biometrics: Theory, Applications and Systems*, pages 346–352. IEEE, 2012.

[3] A. Kumar and Y. Zhou. Human identification using finger images. *IEEE Transactions on Image Processing*, 21(4):2228–2244, 2012.

[4] Y. Li, Y. Yin, and G. Yang. Sensor-oriented feature usability evaluation in fingerprint segmentation. *Optical Engineering*, 52(6):067201–067201, 2013.

[5] F. Liu, Y. Yin, G. Yang, L. Dong, and X. Xi. Finger vein recognition with superpixel-based features. In *2014 International Joint Conference on Biometrics*, pages 1–8. IEEE, 2014.

[6] Y. Lu, S. Xie, Z. Wang, S. Yoon, and D. Park. An available database for the research of finger vein recognition. In *Proceedings of 6th International Congress on Image and Signal Processing*, pages 410–415, 2013.

[7] Y. Lu, S. J. Xie, S. Yoon, J. Yang, and D. S. Park. Robust finger vein roi localization based on flexible segmentation. *Sensors*, 13(11):14339–14366, 2013.

[8] N. Miura, A. Nagasaka, and T. Miyatake. Feature extraction of finger-vein patterns based on repeated line tracking and its application to personal identification. *Machine Vision and Applications*, 15(4):194–203, 2004.

[9] N. Miura, A. Nagasaka, and T. Miyatake. Extraction of finger-vein patterns using maximum curvature points in image profiles. *IEICE TRANSACTIONS on Information and Systems*, 90(8):1185–1194, 2007.

[10] J. K. Pillai, M. Puertas, and R. Chellappa. Cross-sensor iris recognition through kernel learning. *IEEE Transactions on Pattern Analysis and Machine Intelligence*, 36(1):73–85, 2014.

[11] A. Ross and A. Jain. Biometric sensor interoperability: A case study in fingerprints. In *Biometric Authentication*, pages 134–145. Springer, 2004.

[12] A. Ross and R. Nadgir. A thin-plate spline calibration model for fingerprint sensor interoperability. *IEEE Transactions on Knowledge and Data Engineering*, 20(8):1097–1110, 2008.

[13] B. T. Ton and R. N. Veldhuis. A high quality finger vascular pattern dataset collected using a custom designed capturing device. In *2013 International Conference on Biometrics*, pages 1–5. IEEE, 2013.

[14] L. Xiao, Z. Sun, R. He, and T. Tan. Coupled feature selection for cross-sensor iris recognition. In *2013 IEEE Sixth International Conference on Biometrics: Theory, Applications and Systems*, pages 1–6. IEEE, 2013.

[15] J. Yang and Y. Shi. Finger–vein roi localization and vein ridge enhancement. *Pattern Recognition Letters*, 33(12):1569–1579, 2012.

[16] L. Yang, G. Yang, Y. Yin, and R. Xiao. Sliding window-based region of interest extraction for finger vein images. *Sensors*, 13(3):3799–3815, 2013.

[17] Y. Yin, L. Liu, and X. Sun. Sdumla-hmt: a multimodal biometric database. In *In Proceedings of Chinese Conference on Biometric Recognition*, pages 260–268. Springer, 2011.

[18] Y. Zang, X. Yang, X. Jia, N. Zhang, J. Tian, and X. Zhu. A hierarchical registration algorithm for fingerprints from multi-type capture sensors. In *2013 International Conference on Biometrics*, pages 1–6. IEEE, 2013.